Optical and IR Interferometry from Ground and Space
ASP Conference Series, Vol. 3×10^8, *1999*
S.C. Unwin, and R.V. Stachnick, eds.

Atmospheric Fluctuation Measurements with the Palomar Testbed Interferometer

R.P. Linfield

Infrared Processing and Analysis Center, California Institute of Technology, Pasadena, CA 91125

B.F. Lane

Department of Planetary Sciences, California Institute of Technology, Pasadena, CA 91125

M.M. Colavita

Jet Propulsion Laboratory, California Institute of Technology, Pasadena, CA 91109

and the PTI collaboration

Abstract. Delay time series data from the Palomar Testbed Interferometer were used to derive atmospheric turbulence parameters. Data from 18 nights during 1997-1999 are presented. The most significant result is that the power law slope of the delay structure function is much shallower than the three-dimensional Kolmogorov value of 5/3. Measured power law slopes ranged from 1.1 to 1.45. Such sub-Kolmogorov slopes have major, favorable consequences for 'seeing' at infrared wavelengths, and for wide field astrometry with ground-based interferometers.

1. Introduction

The Palomar Testbed Interferometer (PTI) has been used for several years with a 110 m baseline, at 2.2 μm observing wavelength (Colavita et al. 1999). In its single star mode, observations are scheduled for the purpose of amplitude visibility measurements. However, auxiliary data recorded during these observations contains information on atmospheric delay variations.

Our analysis of this archived data had three motivations. The first was to study the physics of atmospheric fluctuations. The second was to better understand the atmospheric error in astronomical measurements (especially those with an interferometer). The third was to look for instrumental error sources by searching for deviations from an atmospheric signature.

2. Interferometer Delay Data

2.1. Method

During PTI operation in single star mode with nominal observing parameters, laser metrology measurements of the delay line position are recorded every 10 msec. Integer cycle ambiguities cause the zero point of these measurements to be arbitrary. However, since the metrology system normally stays locked throughout a night of observing, the measured *differences* are accurate. The delay line is adjusted to track the observed fringes, with a tracking loop time constant of 50 msec.

We restricted our selection of archived data to strong sources ($\Gamma N \geq 250$, where Γ was the fringe visibility and N was the total number of detected photons per 10 msec integration period). With this criterion, the measurement noise on the fringe delays was much smaller than the variation due to the atmosphere. We selected all the data on these strong sources with ≥ 2 scans (typical length of 130 s) on the same night. This ensured a time span > 1000 s (including the gaps between scans) for the data on each source, so that the fitting process (described below) did not corrupt the delay structure functions on time scales < 10 s.

We subtracted a least squares sidereal fit (with a constant term) to all the delay data from a source on each night. The residual delays $\tau(t)$ were used to calculate the delay structure function $D_\tau(\Delta t)$:

$$D_\tau(\Delta t) \equiv \left\langle [\tau(t + \Delta t) - \tau(t)]^2 \right\rangle \tag{1}$$

D_τ was calculated for each 130 s scan, or for 0.05 hr intervals during long scans. A typical structure function is shown in Figure 1. On time scales $<$ 50 msec, the delay tracking loop is not closed, so that the delay line variations do not reflect the atmospheric variations. On time scales of 50–500 msec, the delay tracking loop was closed, and the delay fluctuations over the two telescopes (110 m apart) were almost completely uncorrelated (this is the simplest regime to analyze). A clean power law slope in D_τ was seen in over 95% of the scans. Most of the remaining scans had such a short coherence time (< 20 msec) that the tracking loop was not able to follow short time scale delay variations.

For the scans with a clean power law, a least squares fit over the interval 50-500 msec yielded the power law slope. The slope and intercept were used to calculate the coherence time t_0. This is the time interval over which the measured interferometer delay had a variance of 1 radian^2 (*i.e.* the two aperture variance definition).

2.2. Results

The results for the three nights with the largest number of scans are shown in Figure 2 (1998, Day 180), Figure 3 (1998, Day 291), and Figure 4 (1999, Day 109). A summary of the results for 15 other nights is given in Table 1.

The coherence time varied by factors > 2 during individual nights, consistent with large temporal variations reported with seeing monitors (Martin et al. 1998). The power law slope (β) varied relatively little (< 0.1 *rms*) within one night. In all cases, β was substantially less than the value of 5/3 expected

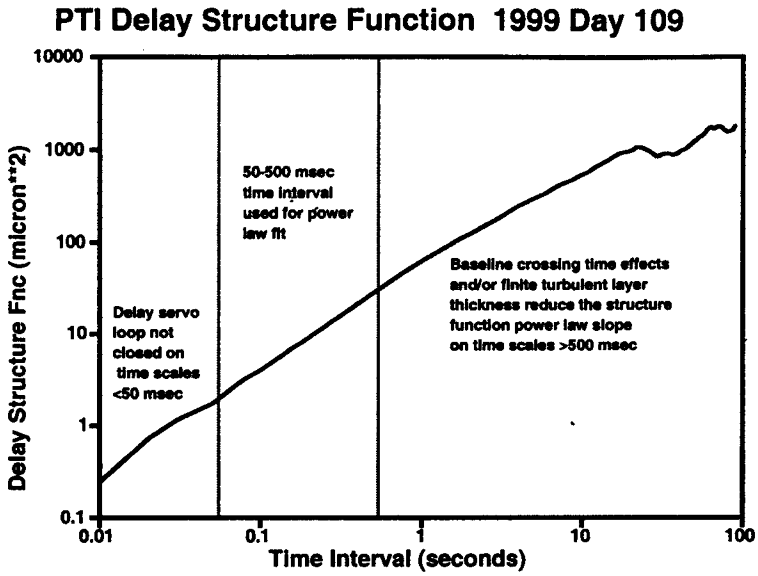

Figure 1. A typical delay structure function, derived from 0.05 hr of PTI data. The fitted values for this structure function are a coherence time of 120 msec, and a power law slope of 1.35

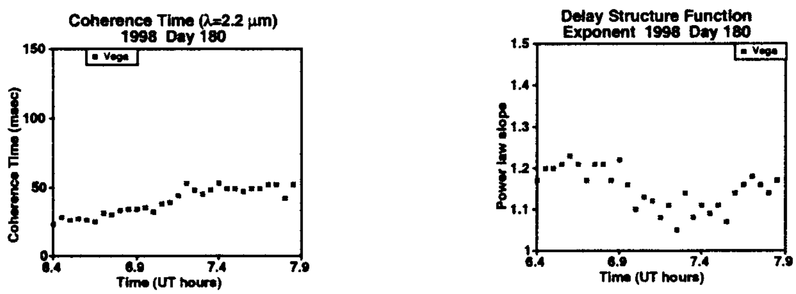

Figure 2. The coherence time and power law slope of the delay structure function, at intervals of 0.05 hr, for 1998 Day 180. The coherence time follows the two aperture variance definition. All these data were from the star Vega.

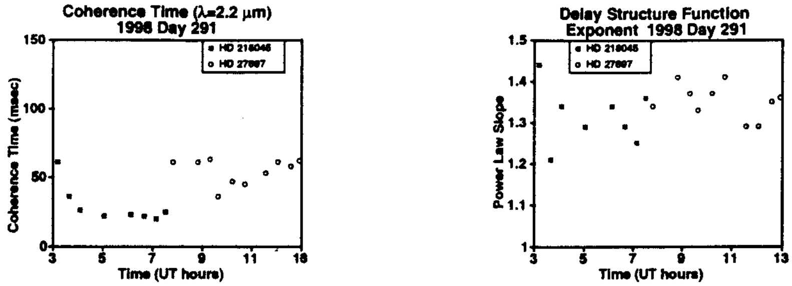

Figure 3. The coherence time and power law slope of the delay structure function, at intervals of 0.05 hr, for 1998 Day 291. The coherence time follows the two aperture variance definition. Data from two stars are shown on the same scale.

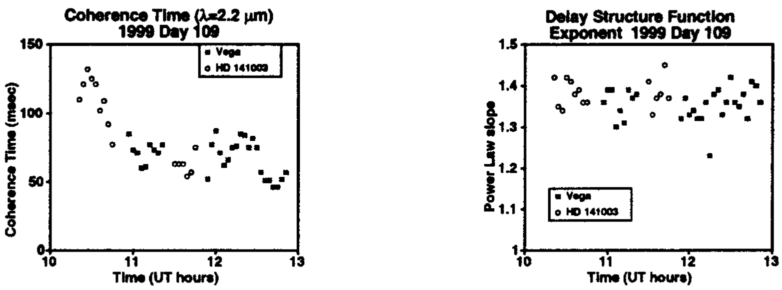

Figure 4. The coherence time and power law slope of the delay structure function, at intervals of 0.05 hr, for 1999 Day 109. The coherence time follows the two aperture variance definition. Data from two stars are shown on the same scale.

Table 1. Summary of atmospheric parameters for additional nights

Year	Day	Number of scans	D_τ exponent	Coherence Time
1997	283	10	1.28	45 msec
1997	295	3	1.31	24 msec
1997	305	4	1.20	27 msec
1997	307	11	1.35	75 msec
1997	309	3	1.28	102 msec
1997	310	4	1.26	74 msec
1997	311	9	1.29	43 msec
1998	243	8	1.44	141 msec
1998	267	6	1.36	60 msec
1998	282	11	1.40	64 msec
1998	283	8	1.40	49 msec
1998	284	7	1.31	79 msec
1998	285	7	1.35	88 msec
1998	287	15	1.40	61 msec
1998	292	15	1.31	81 msec

for three-dimensional Kolmogorov turbulence (Tartarski 1961). Note that the selection criteria restricted our data set to nights with $t_0 > 20$ msec (*i.e.* relatively quiet conditions). Sub-Kolmogorov slopes have previously been reported from data with the Mt. Wilson Infrared Spatial Interferometer (ISI) (Bester et al. 1992). The much longer baseline of PTI (compared to that of ISI) allows easier access to the regime where delay fluctuations over the two telescopes are uncorrelated.

3. Consequences of sub-Kolmogorov Power Laws

Two major consequences of sub-Kolmogorov power law slopes involve the dependence of seeing on wavelength, and the accuracy of wide field astrometric measurements.

For $D_\tau(\Delta t) \propto (\Delta t)^\beta$, the coherence length r_0 varies with wavelength λ as:

$$r_0 \propto \lambda^{2/\beta}$$

The seeing (θ) varies with λ as:

$$\theta \propto \lambda^{1-2/\beta} \tag{2}$$

The difference between a Kolmogorov power law ($\beta = 5/3$) and the typical measured PTI power law ($\beta \approx 1.3$) is dramatic: $\theta \propto \lambda^{-0.2}$ *vs.* $\theta \propto \lambda^{-0.54}$. The seeing at infrared wavelengths is expected to be substantially better than in the visible.

The effect of atmospheric properties on wide field astrometry is illustrated in Figure 5. Here the t_0 and r_0 values measured for 1999 Day 109 at UT 12 were used (star tracker data, not discussed here, were used to determine r_0). For a baseline of 110 m, the delay error is a factor of ≈ 2.5 smaller for $\beta = 1.35$ (the measured value) than for $\beta = 1.67$ (the Kolmogorov value). A detailed characterization of atmospheric statistics will be necessary in order to assign error bars to wide field astrometric data.

References

Bester, M., Danchi, W. C., Degiacomi, C. G., Greenhill, L. J., & Townes, C. H. 1992, ApJ, 392, 357

Colavita, M. M. et al. 1999, ApJ, 510, 505

Martin, F., Tokovinin, A., Ziad, A., Conan, R., Borgnino, J., Avila, R., Agabi, A., and Sarazin, M. 1998, A&A, 336, L49

Tatarski, V. I. 1961, Wave Propogation in a Turbulent Medium, New York: McGraw-Hill

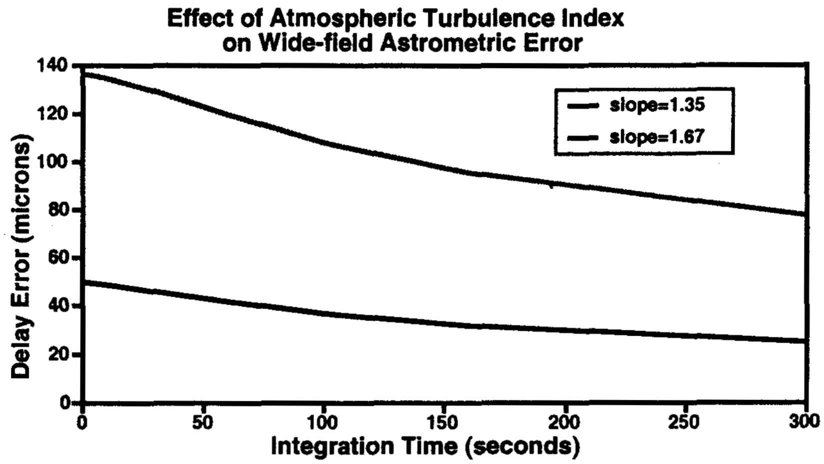

Figure 5. Model calculations of the wide field astrometric error *vs.* integration time, for a 110 m baseline. The coherence time (t_0) and coherence length (r_0) used for both curves were those measured at PTI on 1999, Day 109, UT 12. The only difference was in the power law slope: 1.35 (the measured value on that night) *vs.* 1.67 (the Kolmogorov value)